


Article

Lubrication Mechanisms of a Nanocutting Fluid with Carbon Nanotubes and Sulfurized Isobutylene (CNTs@T321) Composites as Additives

Jiju Guan ^{1,*}, Chao Gao ¹, Zhengya Xu ¹, Lanyu Yang ¹ and Shuiquan Huang ² ¹ College of Mechanical Engineering, Changshu Institute of Technology, Suzhou 215500, China² School of Mechanical Engineering, Yanshan University, Qinhuangdao 066004, China

* Correspondence: guanjjju@cslg.edu.cn

Abstract: Developing high-efficiency lubricant additives and high-performance green cutting fluids has universal significance for maximizing processing efficiency, lowering manufacturing cost, and more importantly reducing environmental concerns caused by the use of conventional mineral oil-based cutting fluids. In this study, a nanocomposite is synthesized by filling sulfurized isobutylene (T321) into acid-treated carbon nanotubes (CNTs) with a liquid-phase wet chemical method. The milling performance of a nanocutting fluid containing CNTs@T321 composites is assessed using a micro-lubrication technology in terms of cutting temperature, cutting force, tool wear, and surface roughness. The composite nanofluid performs better than an individual CNT nanofluid regarding milling performance, with 12%, 20%, and 15% reductions in the cutting force, machining temperature, and surface roughness, respectively. The addition of CNTs@T321 nanocomposites improves the thermal conductivity and wetting performance of the nanofluid, as well as produces a complex lubricating film by releasing T321 during machining. The synergistic effect improves the cutting state at the tool–chip interface, thereby resulting in improved machining performance.

Keywords: carbon nanotube; composites; nanofluids; milling; lubrication mechanism

Citation: Guan, J.; Gao, C.; Xu, Z.; Yang, L.; Huang, S. Lubrication Mechanisms of a Nanocutting Fluid with Carbon Nanotubes and Sulfurized Isobutylene (CNTs@T321) Composites as Additives. *Lubricants* **2022**, *10*, 189. <https://doi.org/10.3390/lubricants10080189>

Received: 22 July 2022

Accepted: 14 August 2022

Published: 19 August 2022

Publisher's Note: MDPI stays neutral with regard to jurisdictional claims in published maps and institutional affiliations.



Copyright: © 2022 by the authors. Licensee MDPI, Basel, Switzerland. This article is an open access article distributed under the terms and conditions of the Creative Commons Attribution (CC BY) license (<https://creativecommons.org/licenses/by/4.0/>).

1. Introduction

Milling is an important processing method in mechanical manufacturing. Modern milling technology has increasingly higher requirements for efficiency, quality, and environmental protection. In the high-speed milling of difficult-to-machine materials, the reasonable selection of cooling and lubrication methods can improve the tool/workpiece friction state and suppress tool wear, which has become a key factor to be considered in cutting process design [1]. Cutting fluid is mainly composed of a base fluid and oily agent, an extreme pressure agent, emulsifier, rust inhibitor, etc., and has the functions of cooling, lubricating, and cleaning. The cost of cutting fluid accounts for 7–17% of the part processing costs, while the cost of cutting tools accounts for 2–4%, according to the investigation in [2]. Various harmful additives appended in cutting fluid have caused many problems, such as environmental pollution, resource consumption, and harm to human health [3]. As a result, continuously developing high-efficiency lubricating additives and new green cutting fluid has universal meaning for maximizing processing efficiency, lowering manufacturing costs, and reducing environmental pollution.

Choi et al. proposed the concept of nanofluid in 1995, which is a suspension formed by dispersing various nanoparticles into a base fluid in a certain proportion [4]. Nanoparticles can put a positive spin on the heat transfer and lubrication performance of the base fluid. As nanotechnology has introduced a new era of rapid development, researchers have recently begun to use nanofluids to achieve efficient cooling and nanotechnology. Nanofluid possesses better thermal conductivity, lower cutting temperature and better tribological conductivity, which can upgrade the lubrication performance of the base fluid

compared to traditional cutting fluid [5,6]. Therefore, nanofluid-based milling processing technology, as an environmentally friendly machining method that achieves cooling and lubrication effects, has good prospects in terms of application. Lee P H and Nam T S used MoS₂ nanofluid in face milling to prove that the use of MoS₂ nanofluid in minimal quantity lubrication (MQL) processing could minimize the cutting force and achieve a better surface quality of a workpiece than the use of conventional cooling methods and cold air cutting [7]. Rahamti et al. used MoS₂ nanofluid to mill an A16061-T6 alloy in a vertical machining center and studied its surface morphology, and the concentration of nanoparticles in basic oil were 0.0%, 0.2%, 0.5% and 1.0 wt%, respectively. The result showed that the surface quality of workpieces was enhanced in regard to the rolling, filling, and polishing of nanoparticles in the processing area. When the concentration of MoS₂ nanoparticles was 0.5 wt%, the surface quality was optimal, while the surface quality declined above 1 wt% [8].

Marcon A and Melkote S prepared water-based graphite nanofluid for the micro-milling of steel H13 under MQL conditions. The results indicated that nanofluid equipped with cooling and lubrication functions could minimize the milling force and had a good polishing effect on the workpiece [9]. Sarah AAD et al. prepared an oil-based nanocutting fluid of onion-like fullerene C60 and carried out research on milling hard aluminum alloy aviation parts. This illustrated that the addition of C60 could reduce the milling force by 21.99% and improve the surface roughness by 46.32%. They believe that C60 acted as a nanoball at the cutting friction interface, thus reducing the cutting force and the tool wear [10]. Sayuti identified the surface morphology of milling A16061-T6 under new SiO₂ nanofluid lubrication, and the concentrations of SiO₂ were 0.0, 0.2, 0.5, and 1.0 wt%. The study showed that the increase in the concentration of SiO₂ nanoparticles promoted the growth of the tool–chip interface protective film, and the film that formed on the machined surface improved the surface quality of the workpiece and reduced the cutting temperature and cutting force [11]. Long T M et al. used MoS₂ nanosheet nanofluid and Al₂O₃/MoS₂ hybrid nanofluid in minimum quantity cooling lubrication (MQCL) hard milling, and the obtained results indicated that better cooling/better effects and good surface quality were achieved [12,13].

Carbon nanotubes (CNTs) are seamless nanotubes formed by monolayer or multi-layer graphite sheets that centrally rotate at a particular helical angle. Every layer of the nanotubes—which are in the shape of a cylinder—consists of a flat hexagon carbon atom attached to three carbon atoms with sp² hybridization [14]. CNTs are an excellent thermally conductive material with good lubrication performance. Their thermal conductivity can reach 6000 W/mK [15], which can improve the heat transfer property of the base fluid and play a similar role in the friction areas of “micro-bearings” [16,17]. Therefore, CNTs are also more suitable as cutting fluid additives. Puneet Sharma et al. used carbon nanotubes to prepare oil-based nanocutting fluids and carried out a study on turning AISI D2 (American Iron and Steel Institute D2) steel under MQL conditions. They identified that, under the action of CNTs, the cutting temperature decreased significantly, the quality of the surface was enhanced, and the tool wear was minimized [18]. The turning of AISI 1040 steel under the lubrication of CNTs nanofluid was analyzed by Rao S N, and the cutting temperature and cutting force were measured, indicating that while the CNT content was below 2%, the temperature and tool wear could be reduced [19]. Sougata Roy et al. studied the turning performance of Al₂O₃ and CNT nanocutting fluids, proving that CNT nanofluids could significantly improve roughness under high-speed turning conditions [20].

As an additive to nanofluids, CNTs have some limitations due to their molecular structure. For instance, they tend to agglomerate and form sediment in the base fluid where the dispersion stability performs inferiorly, incurring the instability of the prepared nanofluid [21]. Though used as a lubricating additive for the deficiency of lubricous molecular groups between molecules, the lubricating efficacy under severe friction conditions is limited. However, CNTs have a special cavity structure with a cavity between 5 and 50 nm. Other substances are permitted to be infused into the cavities of CNTs to structure

a composite under suitable conditions [22,23]. To prepare various composites, various lubricants are filled into CNT cavities, as proposed by the research group. With the introduction of these lubricating compositions into the CNT molecules, the internal filling method improves its lubricating properties compared to the external chemical modification method. In the filling phase, the “end cap” of the CNTs needs to be opened before filling, and hydroxyl and carboxyl groups are bonded to the surface of CNTs at the same time as opening the “end cap” [24,25], fortifying CNTs’ dispersion stability in basic solution. In this paper, the team first fill a typical extreme pressure additive isobutylene sulfide (T321) into CNTs to prepare a CNTs@T321 composite and use it to prepare nanocutting fluid samples and carry out milling processing tests. In the area of cutting, the essence of force and temperature, the workpiece surface roughness and tool wear are comparatively studied, and the machinery of the composite is analyzed. The research findings provide the theoretical basis for the application of CNT nanocutting fluids for milling flat and thin plate parts.

2. Materials and Methods

2.1. Preparation and Characterization of CNTs@T321 Composites

CNTs were purchased from Shanghai Aladdin Reagent Company with 99.9% purity and an inside diameter of 20–50 nm. On account of the large slenderness ratio of these CNTs, which is unfavorable for filling, the CNTs were acidified and shortened first. At the time of acid treating, we first put 20 g of CNTs into 800 mL acid treatment solution (consisting of nitric acid, hydrochloric acid and sulphuric acid; the volume ratio was 3:1:1, with water subdilution 1:1). Then, placing the mixture in a three-necked flask and heating the reflux at 85 °C for 12 h, its magnetic stirring was utilized at a rate of 500 r/min. Then, it was filtered by vacuum and dried at 80 °C; it was then ball grinded for 6 h and acid-treated CNTs were acquired.

Sulfurized isobutylene (T321) was provided by Kangtai Lubricant Additive Co., Ltd. We first dissolved 30 g of T321 with 500 mL of acetone, and then added 90 g acid-treated CNTs. The mixture was placed in a bottle evacuating into a –0.06 Mpa vacuum, and the ultrasonic treatment was applied for 8 h. Then, the filter cake was collected by suction filtration and repeatedly cleaned with acetone to eliminate the T321 that had not been filled, and then the resultant was filtered and the cake was dried at 80 °C. The composites could be obtained by 8 h of ball milling. FEI TECNAI G20 TEM (FEI Company, Hillsboro, OR, USA) was used to observe the microstructure of the nanoparticles, with a 200 kV acceleration voltage in the test. A TG 6300 comprehensive thermal analyzer (Seiko Instruments Inc-SII, Nagano, Japan) was used to test the thermal weight loss characteristic of the composite with a temperature rise of 100–800 °C at a heating rate of 20 °C/min.

2.2. Preparation and Performance Testing of Nanofluids

For nanofluid preparation, surfactants served as dispersers. In this paper, through the preliminary test, a mixture of Tween-80 (TW-80) and dodecylbenzene sulfonate (SDBS) (with mass ratio of 6:4) was used as the surface dispersant. The formulation of water-based nanofluids can be seen in Table 1 below. The nanofluid preparation steps included mixing, mechanically stirring at 50 °C for 30 min, and ultrasonically dispersing for 1 h. After a complete preparation, there were tests for key performances during which three groups were applied to each sample:

Table 1. Formulation of the nanocutting fluids.

Ingredient	Mass Content	Function
Deionization water	97.3 wt%–98.4 wt%	Base Fluid
MWCNTs/composites	0.1 wt%–1.2 wt%	Lubricant additives
Tw-80/SDBS surfactant	0.5 wt%	Activator
Triethanolamine	0.5 wt%	Antirust

The first was the dispersing stability test. We kept every group stationary for 30 days, took 1 mL of the supernatant liquid daily and diluted it by 2 times, and then put it into a cuvette and used a 752 N ultraviolet–visible light photometer to test the absorbency performance of nanofluids at a 500 nm wavelength. The absorbency stability value was used as the basis for estimating the dispersing stability of the nanofluids.

The second was thermal conductivity test where the thermal conductivity of each sample was measured by using a TC3010 L thermal conductivity meter (Xi'an Xiayi Electronic Technology Co., Ltd., Xi'an, China). Each injection was around 30 mL. After the completion of the sample, the instrument automatically determined the thermal conductivity.

Finally, the wettability of the nanofluid was evaluated based on C45 steel surface's contact angle, with measurements from the Kruss DSA25 (KRÜSS Scientific, Hamburg, Germany) instrument. The injected quantity of every drop in the test was 2 μL . For a stable 15 s contact with the surface of the C45 steel, the droplets were in optimum display status throughout the movement test bench and measurement reading.

2.3. Milling Test

The milling test was carried out at the Fadal VMC 3016 L machining center (Fadal Machining Centers, LLC, Murray, GA, USA), as shown in Figure 1a. C45 steel was used as the machining workpiece with the dimensions of 120 mm \times 120 mm \times 80 mm for the rectangular blank; the tool was a TiAlN-coated milling cutter for the test and the milling insert specification was APMT1135PDER-M2/H2 (Chengdu Bangpu Cutting Tools Co., Ltd., Chengdu, China). We used a Kistler 9129A dynamometer (Kistler, Barcelona, Spain) to measure the cutting force, which is a criterion for the resultant force of a three-way cutting force. An RX4006D thermometer (Hangzhou Meacon Automation technology Co., Ltd., Hangzhou, China) was employed to measure the cutting temperature, and a K-type thermocouple (Elitech Co., Ltd., Xuzhou, China) with a diameter of 0.5 mm was buried in the workpiece with small holes, recording the temperature when the machining state was stable.

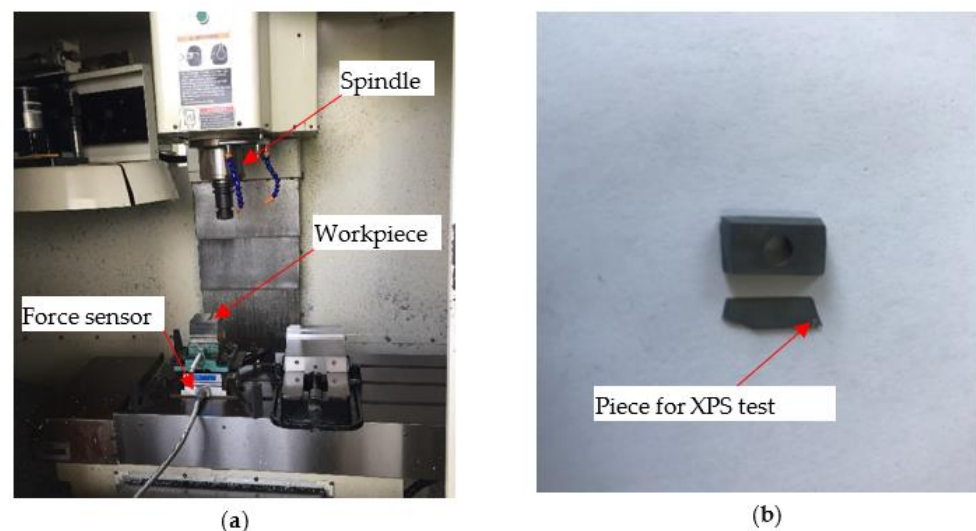


Figure 1. The milling test: (a) equipment used in the test; (b) tool being cut.

First, we investigated the cutting performance of common emulsion, acid-treated CNT nanofluid, and composite nanofluid under MQL conditions, as shown in the A1–A3 groups in Table 2. Second, the milling performance of the nanofluids was investigated when the content of the nanoparticles was 0.02%, 0.04%, 0.06%, 0.08%, 0.1%, 0.3%, 0.5%, 0.7%, 0.9%, and 1.1 wt% under MQL conditions, as shown in the B1–B10 and C1–C10 groups. Moreover, a series of tests of dry cutting in identical cutting conditions were executed, in which the spindle speed was 5000 r/min, the back cutting depth a_p was 0.5 mm, the side cutting depth a_e was 1 mm, the feed per tooth f_z was 0.05 mm, and the total cutting

thickness was 10 mm. We performed three parallel tests for each group of nanofluids. A surface roughness measuring instrument (Beijing Time Yuanfeng Technology Co., Ltd., Beijing, China) was used to measure the surface quality of the workpiece, and the Nikon microscope (Nikon Corporation, Tokyo, Japan) was employed to observe the wear of the tool (*VB*).

Table 2. The cutting test scheme.

Groups	Fluids	Cooling Methods	MQL Conditions
A1	Emulsion (1 wt%)	MQL	Pressure: 0.5 MPa Rate: 40 mL/h Spray distance: 10 mm
A2	CNTs nanofluids (0.1 wt%)		
A3	Composites nanofluids (0.1 wt%)		
B1–B10	CNTs nanofluids (0.02 wt%–1.1 wt%)	MQL	
C1–C10	Composites nanofluids (0.02 wt%–1.1 wt%)		

A metastable lubricating layer may form on the tool face during the milling process, and it is necessary to analyze the composition of the surface lubricating layer. The tools were cut for the analysis under the conditions of dry cutting and emulsifying, CNT nanofluids, and composite nanofluid lubrication, and the thickness of the piece was roughly 1 mm, as shown in Figure 1b. X-ray photoelectron spectroscopy (XPS), an analysis of the wear area binding energy of the essential elements, used the internal standard of 80 eV for the electron flux and 284.8 eV for the binding energy of the contaminated carbon C_{1s} .

3. Results and Discussion

3.1. Characterization of Composites

Figure 2 displays the transmission electron microscopy (TEM) images of the CNTs and composites. Figure 2a shows the hollow tubular structure of the CNTs. Figure 2b presents that several segments of the CNTs@T321 composite sample are filled with T321 in the observed area, proving a successful filling of T321 in the CNTs on the microstructure. The dominating driving force of capillary action for the filling of T321 molecules into the CNT cavity proves that an adequately large force exists in the filler and the nanotube, which can wet each other [26]. Formula (1) is derived from Laplace Equation (2) which gives the relationship of the surface tension and the contact angle at the liquid–solid interface with the pressure difference at the gas–liquid interface [27]:

$$\cos\theta = (\gamma_{sV} - \gamma_{sL})/\gamma \quad (1)$$

$$\Delta P = 2\gamma\cos\theta/r \quad (2)$$

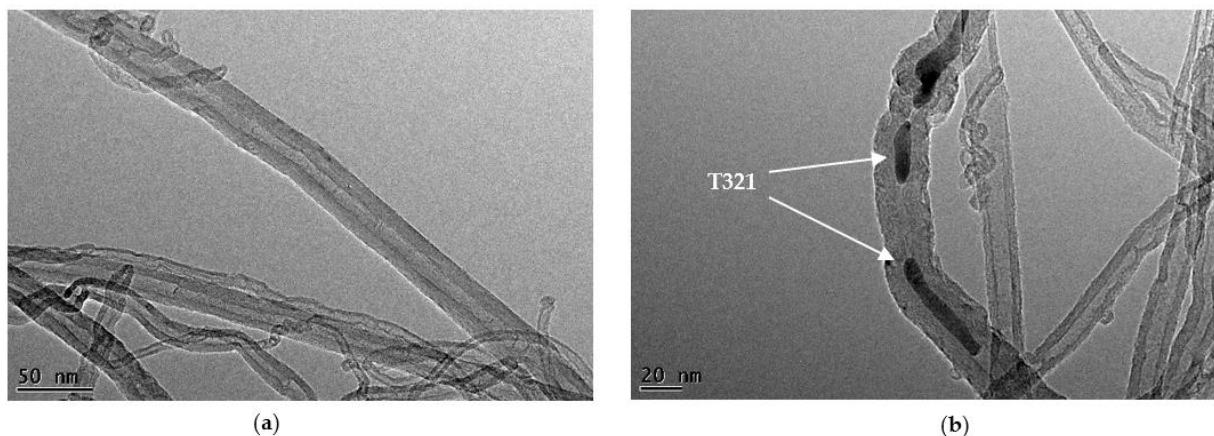


Figure 2. TEM images of nanoparticles: (a) CNTs; (b) composites.

In the formulas, θ is the contact angle of the liquid–solid interface, γ_{sV} is the surface tension of the solid–air interface, γ_{sL} is the surface tension of the solid–liquid interface, γ is the liquid surface tension, and r is the radius of curvature. The determinant of the wetting of CNTs by lubricants is the contact angle θ as capillary action takes place. When $\theta > 90^\circ$, the pressure difference ΔP at the gas–liquid interface is negative, with no wetting occurring. When $\theta < 90^\circ$, only then can infiltration and filling occur. Substances such as water, ethanol, acids, and so forth, with surface tension below 100–200 mN/m are capable of filling in CNTs in specific conditions [28]. The surface tension of T321 is around 97 mN/m, which is further reduced when dissolved in acetone, making it easier to enter CNTs by capillary action. The subsequent drying process evaporates anhydrous ethanol while the T321 in the tube is retained.

In addition, thermal analysis was performed on CNTs, acid-treated CNTs and CNTs@T321 composites, as given in Figure 3. Figure 3a demonstrates that the thermal weight loss properties of CNTs and acidified CNTs were similar with a similar thermal weight loss procedure. However, the thermal weight loss curves of CNT composites had a distinct loss process at a lower temperature as the result of T321 escaping from the object during the heating process. This also proves that T321 exists in CNTs. In accordance with the formula of the latent heat of phase change, the T321 fill rate can be calculated by the following mathematical calculation [29]:

$$\eta = \frac{H_f}{H_p} \times 100\% \quad (3)$$

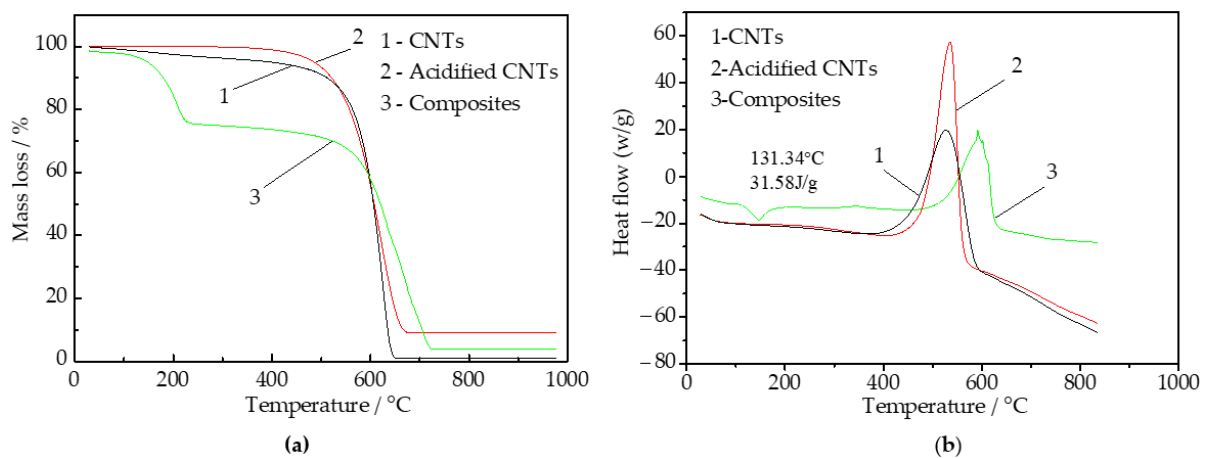


Figure 3. Thermal analysis of CNTs, acidified CNTs and the nanocomposites: (a) TG; (b) DSC.

In this formula, H_f is the phase change heat of T321 that fills in CNTs, J/g, and H_p is the phase change heat of T321 itself, J/g. As the composite in the differential scanning calorimetry (DSC) curve illustrates in Figure 3b, the calculated result of the phase change heat of T321 that fills in CNTs is 31.58 J/g, and the phase change heat of T321 itself is 123.24 J/g under the same heating conditions, so it can be calculated that the filling rate of T321 in CNTs is 25.6%. In addition, the acetone in the filtrate extracted during the composite was evaporated to dryness, and the mass of the remaining T321 was weighed. It can be calculated that the filling rate of the carbon tube was also about 25%, which was basically consistent with the DSC analysis result.

3.2. Physical Performance Test Results of Nanofluids

Figure 4a shows nanofluids with various composite contents, and Figure 4b shows the scanning electron microscope (SEM) image of the nanofluid. It can be seen that the composite had no agglomeration and may have stable dispersion performance. Figure 5a shows the effect of the acid-treated CNTs and composite content on the absorbance of the

nanofluids. It serves to show that a gradual increase in absorbance follows the increase in content with the condition of small nanoparticle content. When the content of the carbon tubes reached a roughly “saturated” 0.3% content, there was an unapparent increase in absorbance, attributed to the deposition of carbon nanotubes that were not dispersed. The dispersion stability of the composite under the same content was better than that of the acid-treated CNTs, which should have been due to the exposure of part of the T321 molecular groups outside the tube. These groups can be combined with surfactants in order to more deeply reinforce the effect of dispersion [30]. Figure 5b illustrates the influence of nanoparticle content on thermal conductivity. The thermal conductivity increases with the increase in content while there is low content, and the base fluid thermal conductivity can be increased by 105% at most. When the content continues increasing, there is a relatively slow increasing trend of thermal conductivity owing to the agglomeration and sedimentation caused by plus nanoparticles with excessive content, which contributes to the decrease in nanoparticles with an obvious effect on heat transfer.

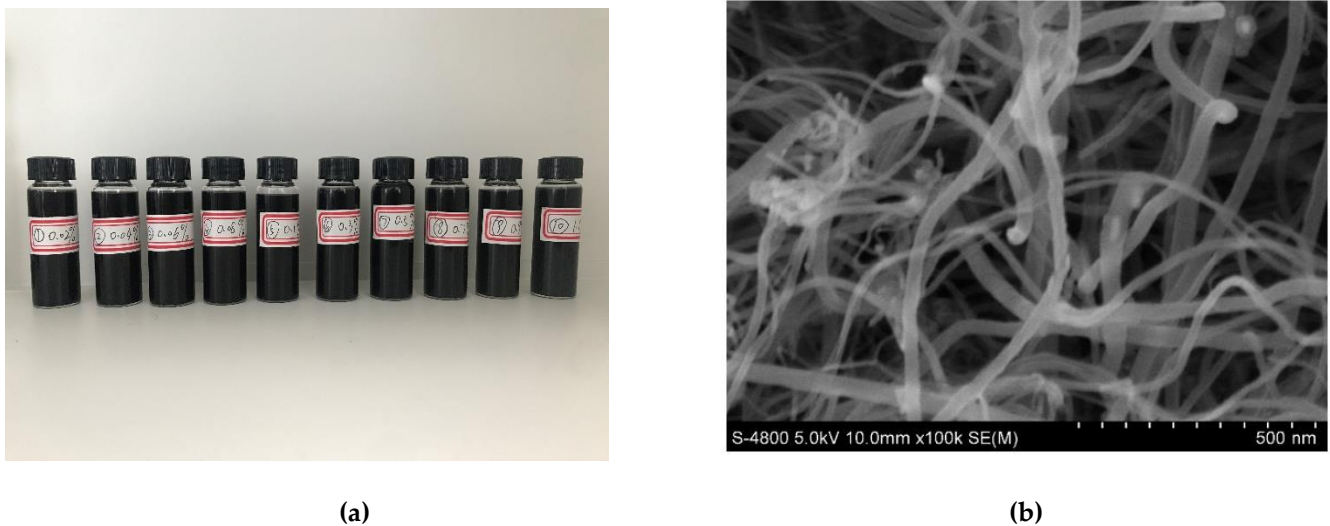


Figure 4. Preparation and SEM image of the nanofluids: (a) nanofluid samples; (b) SEM image of nanofluid.

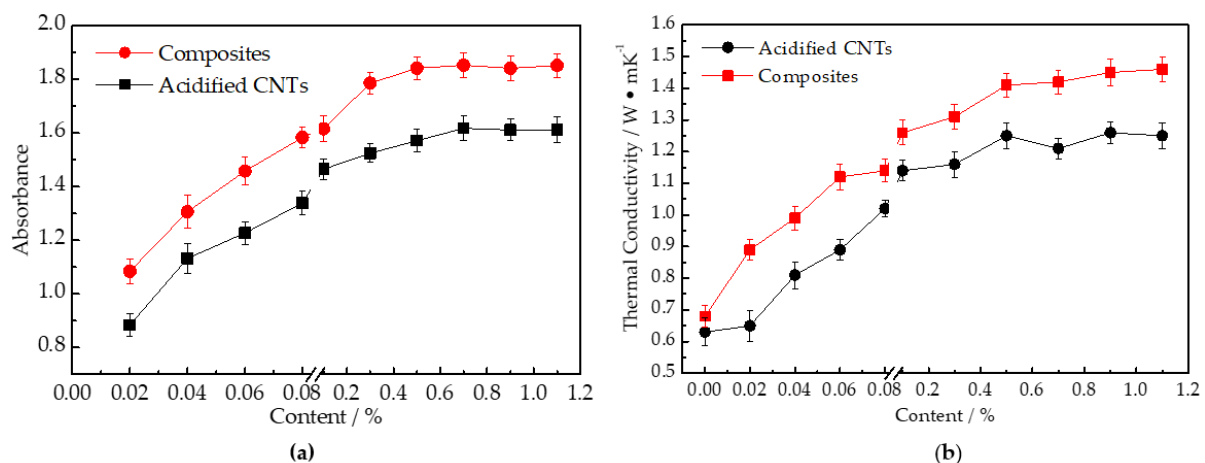


Figure 5. Effects of nanoparticle content on: (a) absorbance; (b) thermal conductivity.

Figure 6a demonstrates the effect of the content on the nanofluids’ wettability when the content of surfactant is 0.5%. Where there is a decrease first, there is an increase later to the contact angle of nanofluids following the increasing nanoparticle content as perceived. Since definite surface activity may be observed with CNTs after treatment

with acid, when they are thoroughly separated in the base fluid, which molecules are repulsed with the nanoparticles and the increasing molecular spacing leads to a reduction in surface tension [31]. In the event that there is an excessively high composite content, worse nanofluid dispersion and viscosity results in an increasing intermolecular force of components, which leads to an increase in contact angle. In addition, in a variety of composite contents, the performance of the composites, compared with those of the acid-treated CNTs in the aspects of wettability and thermal conductivity in relation to surface activity, is stronger and shows more stability in the base solution. Figure 6b shows the nanofluids' viscosity increasing continuously with the increase in content.

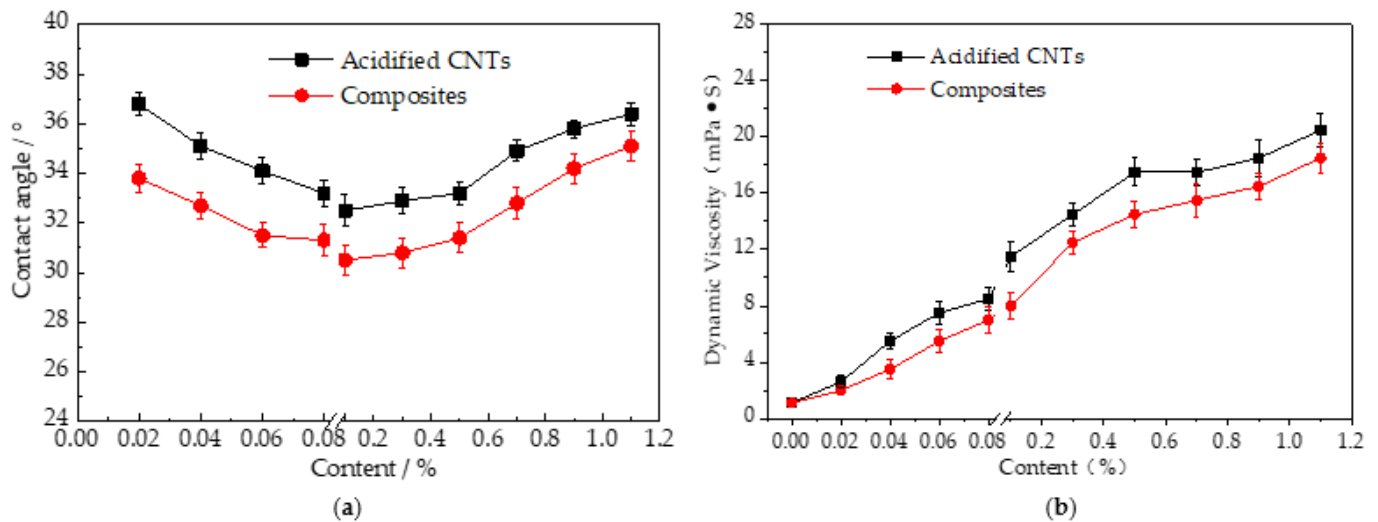


Figure 6. Effects of nanoparticles content on: (a) wettability; (b) viscosity.

3.3. Milling Performance of Different Fluids under MQL Conditions

3.3.1. Force and Temperature in the Cutting Area

The experiment in this paper uses MQL as the supply method of cutting fluid. This is mainly because the provision of cutting fluid presents in mist form in the conditions of MQL with high speed, pressure, and directionality during supply. Penetrating into the cutting area more conductively, the nanofluid has a better anti-friction effect [32,33]. Other studies show an unchanged or increased cutting force in the case of MQL, largely relating to the object of processing and cutting [34,35].

The cutting force is higher when emulsion and CNT nanofluids act in Table 3. An effect of lubrication is produced in the emulsion in which the anti-friction agent is capable of penetrating the cutting area. CNTs can also play a similar role as “micro-bearings” in the cutting area to achieve an effect of definite lubrication [36–38]. However, the molecular structures of CNTs lack effective lubricating groups, and its chemical properties are stable, making a hard reaction in the cutting area. Therefore, its cutting force is relatively high under the same cutting conditions. When the composite nanofluid acts, its cutting force is around 14% lower than that of the emulsion. This is mainly because the composite contains T321 inside, and the composite penetrates it at the time of the cutting process. Additionally, in that case, shear and destroy occur for the composite in the cutting area. The T321 molecules in the composites are released to the cutting area, where the composite is promoted for its anti-friction effect and a cutting force reduction during cutting.

Table 3 demonstrates a comparison between ordinary emulsions and a composite nanofluid whose cutting temperature is lower by almost 33%, chiefly owing to the good thermal conductivity of CNTs. It can be used as an additive that gives a remarkable improvement to the nanofluid's heat transfer capacity and plays an important role in the better heat conduction of the cutting area, which is the reason for the lower nanofluid temperature than the ordinary emulsion. The prepared composite nanofluid compared

with the prepared acid-treated CNT nanofluid possesses a better cooling effect and a better wettability and thermal conductivity of the nanofluid prepared by the composite.

Table 3. Variation in cutting force (F), cutting temperature (T), surface roughness (Ra) and tool wear (VB) under different cutting fluids.

Cutting Fluids	Main Testing Items			
	F/N	$T/^\circ C$	$Ra/\mu m$	$VB/\mu m$
1 wt% Emulsion	218	105	0.939	158
0.1 wt% CNTs	201	85	0.701	134
0.1 wt% Composites	185	71	0.674	105

3.3.2. Tool Wear and Surface Roughness

Table 3 also illustrates the change in the surface quality of the workpiece and the VB value of the tool under the action of various cutting fluids. It points out that the surface roughness under the action of the composite is reduced by 30% and the tool wear is reduced by 34% compared with the ordinary emulsion. It is the extraordinary anti-friction performance of the CNTs that partly separates the tool and workpiece for a cutting force reduction, and the definite polishing on the surface of the workpiece that reduces the surface roughness and retards the tool wear. Under the action of composite nanofluids, the workpiece has the best surface quality and retards the tool wear preferably, which is also due to the better permeability of the composite nanofluid which increases the nanometer entering into the cutting area. In the cutting process, the T321 molecule is released while destruction occurs to the structure of the composite molecule in the cutting area, which brings better lubrication to the composite to obtain a better cutting effect [39].

3.4. Effect of Concentration of Nanoparticle on Milling Properties

3.4.1. Force and Temperature in Cutting Area

The effectiveness of acid-treated CNTs, composite nanoparticle content and cutting area on the cutting force and cutting temperature is demonstrated in Figure 7. It can be seen that with the increase in nanoparticle content, the force and temperature of cutting first decrease and then slowly increase. This is the minimum force and temperature of cutting that can be acquired in the case of the nearly 0.1–0.3% content of the carbon tubes. The lower the nanoparticle content is, the fewer composite particles are in the cutting friction area. This means the relatively modest function of lubrication and heat conduction of the cutting fluid has a limited impact on friction and temperature, with rising improvement in the cutting area. Within a large proportion of nanoparticles, an unsteady dispersion is shown in the base fluid, and the agglomeration and precipitation of the composite are produced, reducing the actual number of nanoparticles that enter the cutting area, leading to the friction increase in the cutting area. Therefore, a more appropriate content of carbon tubes will have a better generation role. Under different contents, a superior effect of lubricating and cooling is generated in the nanofluid that is prepared by the composite. This is because the composite in the base fluid shows better dispersion stability and is more uniform, and consistent prepared nanofluids make for an easier penetration into the cutting area.

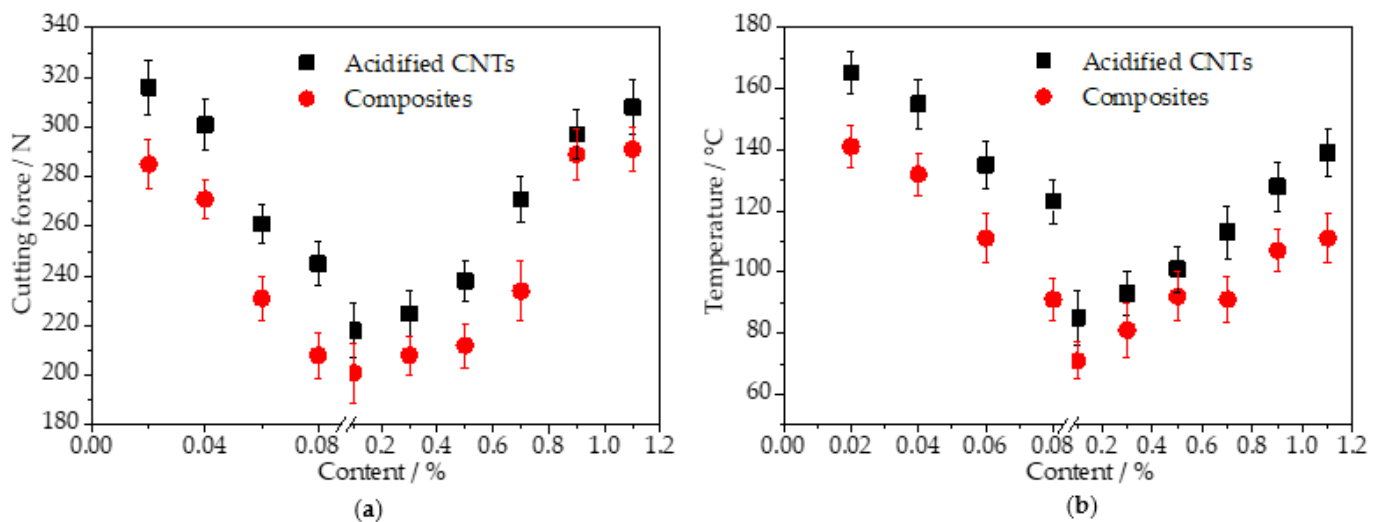


Figure 7. Effect of nanoparticles content: (a) cutting force; (b) cutting temperature.

3.4.2. Tool Wear and Surface Roughness of Workpiece

Figure 8 demonstrates the effect of nanoparticle content on the tool wear and the surface quality of the workpiece. It points out that with the increase in the content of nanoparticles, the surface roughness and the VB value of tool wear also show a tendency to first increase and then decrease. When the content of carbon tubes is about 0.3%, nanofluid can build up workpiece surface quality and slow down the tool wear. With a small proportion of nanoparticle content, there are fewer nanoparticles with limited effects of lubricating and polishing in the cutting area. Nanoparticle composites, with the agglomeration and precipitation that is caused by an excessively large proportion of them, result in fewer nanoparticles entering the cutting area. The nanoparticle decrease causes insufficient lubrication in the cutting area and also brings about the poor surface quality and increased tool wear. Compared with the nanofluid prepared by the acid-treated CNTs, the nanofluid prepared by the composite had a more obvious improvement impact on the tool wear and workpiece surface quality. Primarily, compared with ordinary CNT nanofluids, it is easier to penetrate the cutting processing area with composites. After entering the cutting processing area, nanoparticle composites can have a more sufficient lubrication effect, thereby leading to a reduction in tool wear and an improvement in workpiece surface quality. Next, in the process of cutting, destruction occurs to the composite's molecular structure, and a release of T321 molecules occurs at the cutting area, forming a more sufficient lubrication film. This results in a lower coefficient of friction than ordinary CNTs, and thus the composite has a more obvious lubrication effect on the cutting area, leading to an obvious reduction in tool wear and an improvement in the workpiece surface quality. Lastly, the composite nanofluid has a modified thermal conductivity compared to the CNT nanofluid, and the heat is more easily transferred out during processing, which reduces the temperature of the tool, protects the tool to a certain extent, and reduces wear.

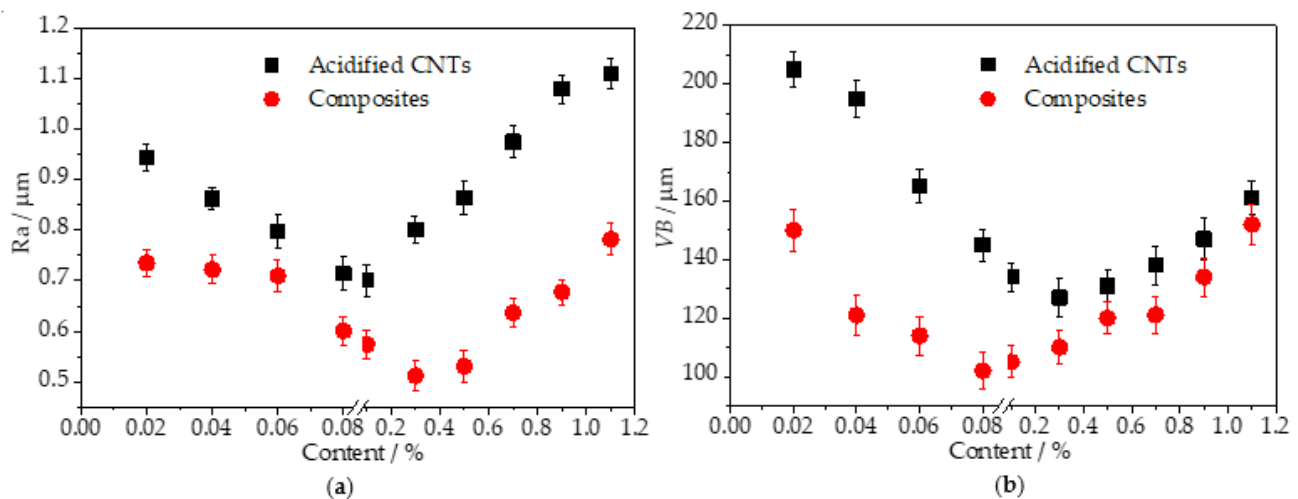


Figure 8. Effect of nanoparticle content: (a) surface roughness; (b) tool wear.

4. Discussion on the Lubrication Mechanism

An analysis has been given by some scholars about the determination of the composition of the stable lubricating film that forms on the worn tool surface [40]. This paper aims to find the major elements of the wear surface of the tool surface under the circumstances of dry cutting or emulsion; CNT nanofluids and composite nanofluids were analyzed by an XPS spectrum to try to give a determination of the process of forming the lubricating layer in the cutting area. C peak separation results of elements, O elements, and S elements are demonstrated in Figure 9. Measurements for every surface of the relative contents of elements C, O, and Fe are listed in Table 4. From Figure 9a,b, we can see that at the time of dry cutting, the C_{1s} and O_{1s} peak shapes on the wear surface of the tool are comparatively simple, mainly belonging to the contaminated carbon, Fe-C bond, and Fe-O bond element types. This surface does not form an effective lubricating layer during dry cutting.

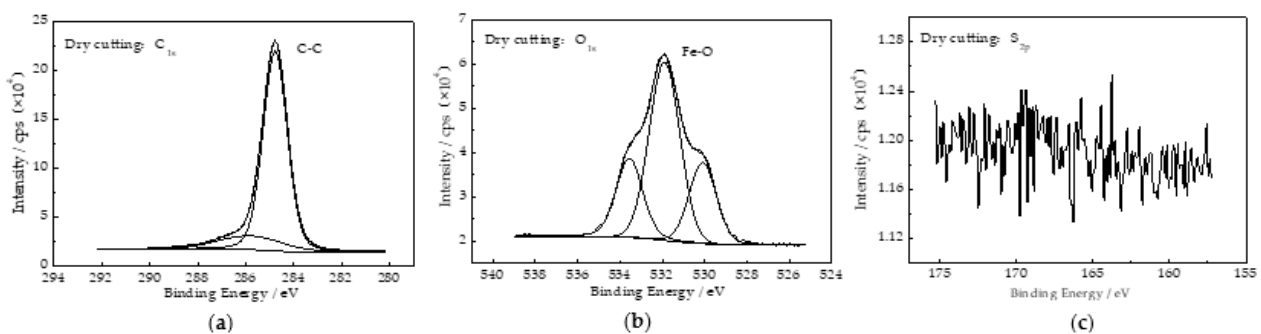


Figure 9. XPS analysis on the worn surfaces of flanks under the condition of dry cutting: (a) C_{1s} ; (b) Fe_{2p} ; (c) S_{2p} .

Table 4. Relative concentration of the main elements on wear surface of the tool.

Elements	Concentration of Main Elements			
	Dry Cutting	Emulsion	CNTs Nanofluids	Composite Nanofluids
C	24.41	41.34	49.47	55.11
O	43.57	40.05	32.69	35.97
Fe	32.02	18.61	17.84	8.92

As shown in Figure 10a,b, under the condition of emulsion lubrication, new peaks of C_{1s} and O_{1s} energy spectrum appear at 289.1 eV and 533.2 eV discriminably, basically be-

longing to C-O bond and C=O bond [41,42], which shows the effect of the lateral adsorption of the active lubricating components in the emulsion. Visible peaks of the S element appear at the tool wear surface with the micro-lubricating emulsion in comparison to the condition of dry cutting. This indicates that the emulsion is sulfur-added, which is related to the appearance of S_{2p} peaks at around 162.2 eV and 168.4 eV, showing that they remain with the Fe-S bond and S-O bond in several instances. The adsorption of active ingredients in the emulsion during the cutting is proven in Table 4, which illustrates a 70% content increase in C in comparison with the wear surface of the tool under the condition of dry cutting.

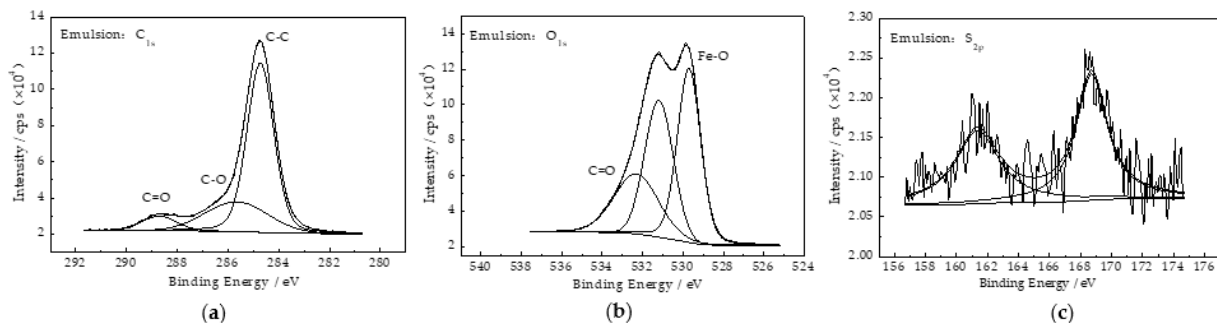


Figure 10. XPS analysis on the worn surfaces of flanks under the lubrication of emulsion: (a) C_{1s} ; (b) Fe_{2p} ; (c) S_{2p} .

As shown in Figure 11a,b, with the CNT nanofluid function, the C_{1s} and O_{1s} energy spectra of the flank wear area are split. It may be inferred that 284.6 eV, 285.8 eV, 288.2 eV and 291.2 eV are the energy spectra of four small peak shapes attributed to C_{1s} . Being part of the carbon species, the first three fitting peaks belong to C-C, C-O and C=O, comparatively, and the last one of 289.1 eV is more intricate, such as polymer- $[C-C]_n^-$, and so forth [42]. A small peak appears near 534.3 eV on the O_{1s} energy spectrum, proving that CNTs form a more complicated lubricating ingredient when acting. Table 4 gives a comparison with the worn surface of dry cutting; the content of the C element on the CNT nanocutting fluid surface has doubled, proving that CNTs also have components of lubrication that form in the cutting area. The “micro-bearings” role is predominantly played by CNTs in the cutting friction process, while some of them break with the frictional shear action. A visible increase can be seen in C element’s relative content, which is led by the result of CNT depositing and adsorption affecting the enhancement of the anti-friction effect of the composite.

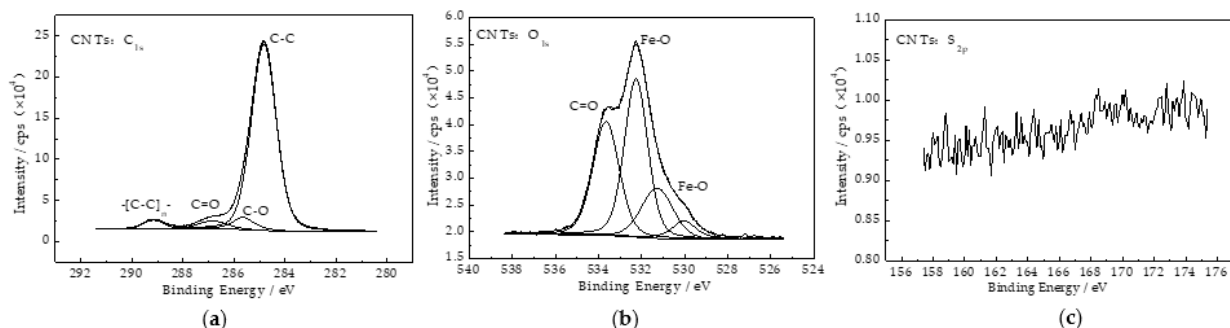


Figure 11. XPS analysis on the worn surfaces of flanks under the lubrication of CNT nanofluids: (a) C_{1s} ; (b) Fe_{2p} ; (c) S_{2p} .

Figure 12b exhibits that when the nanofluid prepared by the composite acts as lubrication, the peak shape of the C_{1s} energy spectrum is similar to that in Figure 11a, but the relative area of the peak shape of the fitting peak C=O is larger, with which $[C-C]_n^-$ is smaller. The O_{1s} spectrum is relatively similar to that in Figure 11b, but with a wider peak

shape, and the sub-peaks are attributed to more prominent C-O and C=O, which proves that a similarity exists between the composite lubricating layer and CNTs in the process of forming. Then, a certain influence on the forming lubrication layer of CNTs may be affected by the discharge of T321 in the process of cutting. Being exposed to the nanofluid of the composite, the S_{2p} spectrum on the worn surface also has two peaks appearing at 162.4 eV and 168.2 eV distinctly, demonstrating that a vulcanized film is formed. Table 4 figures that the C element on the worn surface of the composite nanofluid lubrication is further increasing, the relative Fe element content is minimum, and the O content is between that of T321 and CNTs separately. This proves that a more abundant lubricating film is formed on the wear surface when the CNTs@T321 composite acts. It may be seen that the lubricating layer, which is composed of a vulcanized film, is formed between T321 and CNTs when the action happens separately. Figure 13 shows a model illustrating the lubrication mechanism of the composite at the cutting zone [43]. During cutting, T321 is released from the composites, and the active groups in T321 form a lubricating film through physical or chemical adsorption, relieving the friction at both the tool–chip and tool–workpiece interfaces. This reduces the cutting force and cutting temperature, and hence improves the surface quality. Meanwhile, CNTs are broken due to the action of cutting, and the generated fragment groups such as R-CH₂- and R-O- are adsorbed on the frictional interfaces, generating a lubricative film to help improve the interfacial lubrication. In addition, the composites can also act like micro bearings to lower the sliding friction, resulting in improved cutting performance.

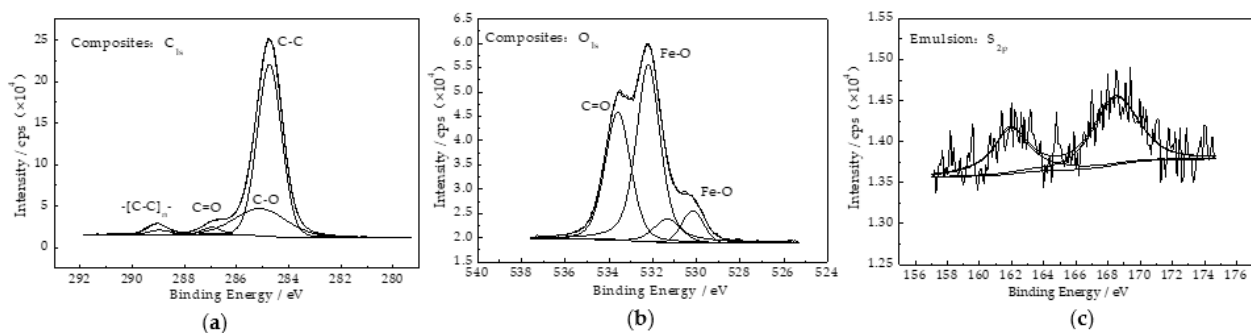


Figure 12. XPS analysis on the worn surfaces of flanks under the lubrication of composite nanofluids: (a) C_{1s} ; (b) Fe_{2p} ; (c) S_{2p} .

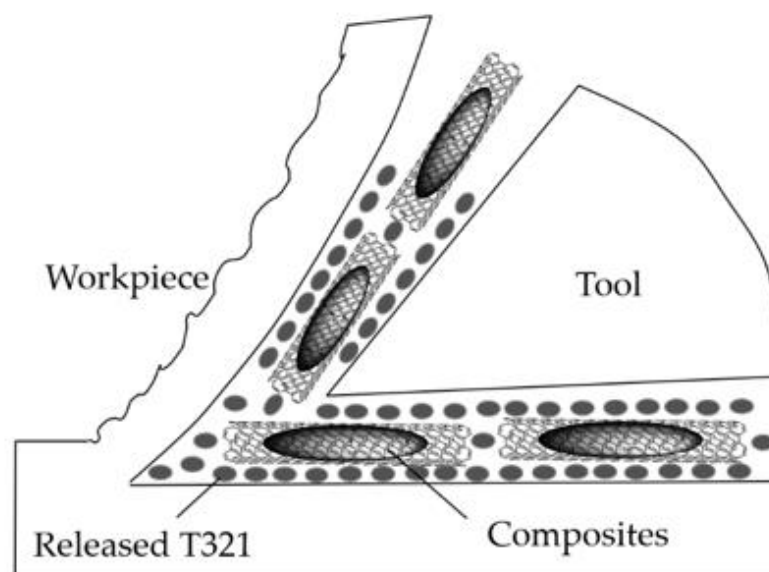


Figure 13. A model of the lubrication mechanism of the composites.

5. Conclusions

(1) CNTs@T321 nanocomposites were synthesized with an approximate fill rate of T321 of 25%. The addition of the synthesized nanocomposites significantly improved the dispersion stability, heat transferability and wettability of the nanofluid;

(2) The application of the developed CNTs@T321 nanofluid generated lower cutting force and cutting temperature, as well as better machined surface quality and tool life, with 12%, 20%, 15%, and 15% improvements compared with the commercially available emulsion;

(3) During cutting, CNTs@T321 composite nanofluids produced a complex protective film containing a T321-based lubricating layer and a CNT-related tribo-layer. The synergistic lubrication effect of the protective film improved the friction state at both the tool–chip and tool–workpiece interfaces, thereby resulting in improved machining performance;

(4) This research offers an effective and practical way to synthesize metalworking fluids for the optimal performance and sustainable machining of difficult-to-machine materials.

Author Contributions: Conceptualization, J.G. and S.H.; methodology, Z.X.; software, C.G.; validation, J.G., C.G. and L.Y.; formal analysis, L.Y.; investigation, L.Y.; resources, S.H.; data curation, C.G.; writing—original draft preparation, C.G.; writing—review and editing, J.G.; visualization, L.Y.; supervision, Z.X.; project administration, L.Y.; funding acquisition, J.G. and S.H.; All authors have read and agreed to the published version of the manuscript.

Funding: This research was financially supported by the Youth Science Foundation Program, Natural Science Foundation of China, with the project number of NSFC 51805345. And the Natural Science Foundation of Hebei Province, with the project number of E2022203123.

Data Availability Statement: Not applicable.

Conflicts of Interest: The authors declare no conflict of interest.

References

- Bruce, R.W. *Handbook of Lubrication and Tribology: Theory and Design*, 2nd ed.; CRC Press: Boca Raton, FL, USA, 2012.
- Klocke, F.; Eisenblatter, G. Dry Cutting. *Ann. CIRP* **1997**, *46*, 519–526. [[CrossRef](#)]
- Mirer, F.E. New Evidence on The Health Hazards and Control of Metalworking Fluids Since Completion of the Osha Advisory Committee Report. *Am. J. Ind. Med.* **2010**, *53*, 792–801. [[CrossRef](#)]
- Choi, S.U.S.; Eastman, J.A. Enhancing Thermal Conductivity of Fluids with Nanoparticles. In Proceedings of the 1995 ASME International Mechanical Engineering Congress & Exposition, San Francisco, CA, USA, 12–17 November 1995; Volume 66, pp. 99–105.
- Kilincarslan, S.K.; Cetin, M.H. Improvement of the Milling Process Performance by Using Cutting Fluids Prepared with Nano-Silver and Boric Acid. *J. Manuf. Process.* **2020**, *56*, 707–717. [[CrossRef](#)]
- Kumar, A.S.; Paul, S.D.S. Tribological Characteristics and Micro-milling Performance of Nanoparticle Enhanced Water Based Cutting Fluids in Minimum Quantity Lubrication. *J. Manuf. Process.* **2020**, *56*, 766–776. [[CrossRef](#)]
- Lee, P.H.; Nam, T.S.; Li, C.J.; Lee, S.W. Experimental Study on Meso-Scale Milling Process Using Nanofluid Minimum Quantity Lubrication. *Trans. Korean Soc. Mech. Eng. A* **2010**, *34*, 1493–1498. [[CrossRef](#)]
- Rahmati, B.; Sarhan, A.A.D.; Sayuti, M. Morphology of Surface Generated by End Milling AL6061-T6 Using Molybdenum Disulfide (MoS₂) Nano-lubrication in End Milling Machining. *J. Clean Prod.* **2013**, *66*, 685–691. [[CrossRef](#)]
- Marcon, A.; Melkote, S.; Kalaitzidou, K.; Debra, D. An Experimental Evaluation of Graphite Nanoplatelet Based Lubricant in Micro-Milling. *CIRP Ann.-Manuf. Technol.* **2010**, *59*, 141–144. [[CrossRef](#)]
- Sayuti, M.; Sarhan, A.A.D. Cutting Force Reduction and Surface Quality Improvement in Machining of Aerospace Duralumin AL-2017-T4 Using Carbon Onion Nano-Lubrication System. *Int. J. Adv. Manuf. Technol.* **2013**, *65*, 1493–1500. [[CrossRef](#)]
- Sayuti, M.; Erh, O.M.; Sarhan, A.A.D.; Hamdi, M. Investigation on the Morphology of The Machined Surface in End Milling of Aerospace AL6061-T6 for Novel Uses of SiO₂ Nano Lubrication System. *J. Clean Prod.* **2013**, *66*, 655–663. [[CrossRef](#)]
- Pham, Q.D.; Tran, M.D.; Ngo, M.T.; Tran, T.L.; Nguyen, V.T. Improvement in the Hard Milling of AISI D2 Steel under the MQCL Condition Using Emulsion-Dispersed MoS₂ Nanosheets. *Lubricants* **2020**, *8*, 62.
- Duc, T.M.; Long, T.T.; Tuan, N.M. Novel Uses of Al₂O₃/MoS₂ Hybrid Nanofluid in MQCL Hard Milling of Hardox 500 Steel. *Lubricants* **2021**, *9*, 45. [[CrossRef](#)]
- Iijima, S. Helical Microtubes of Graphitic Carbon. *Nature* **1991**, *354*, 56–58. [[CrossRef](#)]
- Clancy, T.C.; Gates, T.S. Modeling of Interfacial Modification Effects on Thermal Conductivity of Carbon Nanotube Composites. *Polymer* **2006**, *47*, 5990–5996. [[CrossRef](#)]
- Sharma, A.K.; Arun, K.T.A.K.; Dixit, A.R. Effects of Minimum Quantity Lubrication (MQL) in Machining Processes Using Conventional and Nanofluid Based Cutting Fluids: A Comprehensive Review. *J. Clean Prod.* **2016**, *127*, 1–18. [[CrossRef](#)]

17. Prabhu, S.; Vinayagam, B.K. AFM Investigation in Grinding Process with Nanofluids Using Taguchi Analysis. *Int. J. Adv. Manuf. Technol.* **2012**, *60*, 149–160. [[CrossRef](#)]
18. Sharma, P.; Sidhu, B.S.; Sharma, J. Investigation of Effects of Nanofluids on Turning of AISI D2 Steel Using Minimum Quantity Lubrication. *J. Clean Prod.* **2015**, *108*, 72–79. [[CrossRef](#)]
19. Rao, S.N.; Satyanarayana, D.B.; Venkatasubbaiah, D.K. Experimental Estimation of Tool Wear and Cutting Temperatures in MQL Using Cutting Fluids with CNT Inclusion. *Int. J. Eng. Sci.* **2011**, *4*, 2928–2931.
20. Roy, S.; Ghosh, A. High-Speed Turning of AISI 4140 Steel Using Nanofluid Through Twin Jet SQL System. *ASME Int. Manuf. Sci. Eng. Conf.* **2013**, *55461*, 10–14.
21. Wang, P.; Zhang, D. Effect of Molecular Structure on Dispersion of Carbon Nanotubes by Natural Organic Matter Surrogates. *China Environ. Sci.* **2018**, *38*, 3429–3436.
22. Yuba, R.P.; Li, W.Z. Synthesis, Properties, and Applications of Carbon Nanotubes Filled with Foreign Materials: A Review. *Mater. Today Phys.* **2018**, *7*, 7–34.
23. Sinha, A.K.; Hwang, D.W.; Hwang, L.P. A Novel Approach to Bulk Synthesis of Carbon Nanotubes Filled with Metal by A Catalytic Chemical Vapor Deposition Method. *Chem. Phys. Lett.* **2000**, *332*, 455–460. [[CrossRef](#)]
24. Wang, G.J.; Qu, Z.H. Modification of Carbon Nanotubes by Chemical Reaction. *Prog. Chem.* **2006**, *18*, 1305–1312.
25. Connell, M.J.; Boul, P.; Ericson, L.M. Reversible Water-Solubilization of Single-Walled Carbon Nanotubes by Polymer Wrapping. *Chem. Phys. Lett.* **2001**, *342*, 265–271. [[CrossRef](#)]
26. Ajayan, P.M.; Iijima, S. Capillarity Induced Filling of Carbon Nanotubes. *Nature* **1993**, *361*, 333–335. [[CrossRef](#)]
27. Dujardin, E.; Ebbesen, T.W.; Hiura, H. Capillarity of Carbon Nanotubes. *Science* **1994**, *265*, 1850–1852. [[CrossRef](#)] [[PubMed](#)]
28. Pederson, M.R.; Broughton, J.Q. Nano-Capillarity in Fullerene Tubules. *Phys. Rev. Lett.* **1992**, *69*, 2689–2692. [[CrossRef](#)]
29. Kumar, P.G.; Renuka, M.; Velraj, R. Thermal and Electrical Conductivity Enhancement of Solar Glycol-Water Mixture Containing MWCNTs. *Fuller. Nanotub. Car. N.* **2018**, *26*, 871–879.
30. Guan, J.J.; Wang, J.; Lv, T.; Xu, X.F. Dispersion Stability and Enhanced Heat Transfer of Cutting Use Nanofluids Prepared by Composite of Carbon Nanotubes and Dialkyl Pentasulfide. *Mater. Res. Express* **2019**, *8*, 085633.
31. Nurettin, S.; Muammer, K. Stabilization of the Aqueous Dispersion of Carbon Nanotubes Using Different Approaches. *Therm. Sci. Eng. Prog.* **2018**, *8*, 411–417.
32. Dhar, N.; Islam, M.; Islam, S.; Mithu, M. An Experimental Investigation on Effect of Minimum Quantity Lubrication in Machining AISI 1040 Steel. *Int. J. Mach. Tools Manuf.* **2007**, *47*, 748–753. [[CrossRef](#)]
33. Bikash, C.B.; Chetana, D.S.; Sudarsan, G.P.; Venkateswara, R. Spread Ability Studies of Metal Working Fluids on Tool Surface and Its Impact on Minimum Amount Cooling and Lubrication Turning. *J. Mater. Process. Tech.* **2017**, *244*, 1–16. [[CrossRef](#)]
34. Xu, J.; Yamada, K.; Sekiya, K. Study of Comparing Cutting Force Signal Features for Dry, Air Cooling and Minimum Quantity Lubrication (MQL) Drilling. *J. Adv. Mech. Des. Syst.* **2017**, *11*, JAMDSM0030. [[CrossRef](#)]
35. Xia, J.; Li, B.Z.; Zhang, X.P. The Effects of Minimum Quantity Lubrication (MQL) on Machining Force, Temperature, And Residual Stress. *Int. J. Precis. Eng. Man.* **2014**, *15*, 2443–2451.
36. Zhang, Y.B.; Li, C.H.; Jia, D.Z.; Li, B.K. Experimental Study on The Effect of Nanoparticle Concentration on The Lubricating Property of Nanofluids for MQL Grinding of Ni-Based Alloy. *J. Mater. Process. Tech.* **2016**, *232*, 100–115. [[CrossRef](#)]
37. Chinchankar, S.; Kore, S.S.; Hujare, P.A. Review on Nanofluids in Minimum Quantity Lubrication Machining. *J. Manuf. Process.* **2021**, *68*, 56–70. [[CrossRef](#)]
38. Abubakr, M.; Hegab, H.; Osman, T.A.; Elharouni, F.; Kishawy, H.A.; Esawi, A.M. Carbon Nanotube-Based Nanofluids: Properties and Applications. In *Handbook of Carbon Nanotubes*; Springer International Publishing: Cham, Switzerland, 2022.
39. Guan, J.J.; Liu, D.L.; Wang, Y.; Feng, B.H.; Xu, X.F. Tribological Properties of Nanofluid Prepared by Composite of Multi-Walled Carbon Nanotube and Oleic Acid. *Tribology* **2020**, *40*, 290–299.
40. Dosbaeva, G.K.; Hakim, M.A.; Shalaby, M.A. Cutting Temperature Effect on PCBN And CVD Coated Carbide Tools in Hard Turning of D2 Tool Steel. *Int. J. Refract. Met. H* **2015**, *50*, 1–8. [[CrossRef](#)]
41. Briggs, D. *Surface Analysis of Polymers by XPS and Static SIMS*, 1st ed.; Cambridge University Press: Cambridge, NY, USA, 1998.
42. Rashi, G.; Amzad, K.; Om, P.K. Fatty Acid-Derived Ionic Liquids as Renewable Lubricant Additives: Effect of Chain Length and Unsaturation. *J. Mol. Liq.* **2020**, *301*, 112322.
43. Hegab, H.; Umer, U.; Esawi, A.; Kishawy, H.A. Tribological Mechanisms of Nano-Cutting Fluid Minimum Quantity Lubrication: A Comparative Performance Analysis Model. *Int. J. Adv. Manuf. Technol.* **2020**, *108*, 3133–3139. [[CrossRef](#)]